Radiology

ORIGINAL RESEARCH • THORACIC IMAGING

Use of Elastic Registration in Pulmonary MRI for the Assessment of Pulmonary Fibrosis in Patients with Systemic Sclerosis

Guillaume Chassagnon, MD • Charlotte Martin, MD* • Rafael Marini, MSc • Maria Vakalopolou, PhD • Alexis Régent, MD, PhD • Luc Mouthon, MD, PhD • Nikos Paragios, PhD • Marie-Pierre Revel, MD, PhD*

From the Department of Radiology, Groupe Hospitalier Cochin-Hôtel Dieu, AP-HP, Université Paris Descartes, 27 Rue du Faubourg Saint-Jacques, 75014 Paris, France (G.C., C.M., M.P.R.); Center for Visual Computing, École CentraleSupélec, Gif-sur-Yvette, France (G.C., M.V., N.P.); TheraPanacea, Pépinière Santé Cochin, Paris, France (R.M., N.P.); and Department of Internal Medicine, Reference Center for Rare Systemic Autoimmune Diseases of Île de France, Hôpital Cochin, AP-HP, Université Paris Descartes, 27 Rue du Faubourg Saint-Jacques, 75014 Paris, France (A.R., L.M.). Received September 11, 2018; revision requested October 23; final revision received December 25; accepted January 14, 2019. **Address correspondence to** M.P.R. (e-mail: *marie-pierre.revel@aphp.fr*).

* G.C. and C.M. contributed equally to this work.

Conflicts of interest are listed at the end of this article.

See also the editorial by Biederer in this issue.

Radiology 2019; 291:487–492 • https://doi.org/10.1148/radiol.2019182099 • Content codes: CH MR

Background: Current imaging methods are not sensitive to changes in pulmonary function resulting from fibrosis. MRI with ultrashort echo time can be used to image the lung parenchyma and lung motion.

Purpose: To evaluate elastic registration of inspiratory-to-expiratory lung MRI for the assessment of pulmonary fibrosis in study participants with systemic sclerosis (SSc).

Materials and Methods: This prospective study was performed from September 2017 to March 2018 and recruited healthy volunteers and participants with SSc and high-resolution CT (within the previous 3 months) of the chest for lung MRI. Two breath-hold, coronal, three-dimensional, ultrashort–echo-time, gradient-echo sequences of the lungs were acquired after full inspiration and expiration with a 3.0-T unit. Images were registered from inspiration to expiration by using an elastic registration algorithm. Jacobian determinants were calculated from deformation fields and represented on color maps. Similarity between areas with marked shrinkage and logarithm of Jacobian determinants less than −0.15 were compared between healthy volunteers and study participants with SSc. Receiver operating characteristic curve analysis was performed to determine the best Dice similarity coefficient threshold for diagnosis of fibrosis.

Results: Sixteen participants with SSc (seven with pulmonary fibrosis at high-resolution CT) and 11 healthy volunteers were evaluated. Areas of marked shrinkage during expiration with logarithm of Jacobian determinants less than −0.15 were found in the posterior lung bases of healthy volunteers and in participants with SSc without fibrosis, but not in participants with fibrosis. The sensitivity and specificity of MRI for presence of fibrosis at high-resolution CT were 86% and 75%, respectively (area under the curve, 0.81; $P = .04$) by using a threshold of 0.36 for Dice similarity coefficient.

Conclusion: Elastic registration of inspiratory-to-expiratory MRI shows less lung base respiratory deformation in study participants with systemic sclerosis–related pulmonary fibrosis compared with participants without fibrosis.

Online supplemental material is available for this article.

High-resolution CT plays an important role in the detection and follow-up of lung fibrosis (1). It is especially important in patients with systemic sclerosis (SSc), where pulmonary involvement represents the leading cause of death and is initially clinically silent. High-resolution CT analysis only provides morphologic information and the activity of fibrosis cannot be evaluated. In addition, high-resolution CT is not sensitive to subtle changes in lung morphology or changes in pulmonary function. This is the reason why new imaging biomarkers of pulmonary fibrosis are needed.

MRI is a radiation-free technique, and acquisitions can be safely repeated at different portions of the respiratory cycle. This is important when testing new methods of evaluation. The development of sequences with ultrashort echo times compensate for the low proton density and very short transverse relaxation time (or T2*) of the lung parenchyma (2–6). MRI may be used to analyze respiratory movements by coupling MRI dynamic acquisition and registration methods (7). Elastic registration algorithms are designed to find the transformation, allowing a source image to match with a target image. Thus, the difference between the two images can be quantified.

We hypothesized that elastic registration could be used to evaluate and quantify the local lung deformation between inspiratory (source image) and expiratory lung MRI (target image), and to compare lung deformation patterns in healthy volunteers and study participants with known lung fibrosis documented at high-resolution CT. As a demonstration of these methods, we studied participants with SSc, known to have a high prevalence of pulmonary fibrosis. Thus, the purpose of this study was to evaluate the feasibility of elastic registration of

Abbreviation

SSc = systemic sclerosis

Summary

Elastic registration of inspiratory and expiratory MRI revealed qualitative and quantitative differences in lung deformation in study participants with systemic sclerosis compared with healthy volunteers.

Key Points

- Areas of marked shrinkage during expiration MRI were found in the posterior lung bases of healthy volunteers and in participants with systemic sclerosis without fibrosis, but not in participants with fibrosis.
- The sensitivity and specificity of MRI for presence of fibrosis at high-resolution CT were 86% and 75%, respectively (area under the curve, 0.81)

inspiratory-to-expiratory lung MRI for the assessment of pulmonary fibrosis in study participants with SSc.

Materials and Methods

Two authors (R.M. and N.P.) are employees of TheraPanacea (Paris, France). They provided support for the elastic registration process but had no control of the data or statistics.

Study Participants

This prospective single-center cohort study was approved by the Sud-Ouest et Outre-Mer I ethics committee (study number, 2017-A00961–52) and registered at ClinicalTrials.gov (registration number, NCT03207997). All participants provided written informed consent. From September 2017 to March 2018, all consecutive participants with SSc referred for cardiac MRI as part of their routine follow-up at Cochin University Hospital (Paris, France) were asked to give their consent for undergoing additional lung MRI sequences. Included participants were at least 18 years old with a confirmed diagnosis of SSc based on 2013 American College of Rheumatology and European League Against Rheumatism criteria (8) and recent (within the previous 3 months) pulmonary function tests and high-resolution CT performed with standard parameters (section thickness, 0.625 mm to 1.25 mm; sharp kernel; matrix, 512 × 512). Exclusion criteria were exacerbation of pulmonary fibrosis, orthopnea, and inability to perform a 17-second breath hold. A group of healthy volunteers also underwent lung MRI.

MRI Sequences

All MRIs were performed with a 3.0-T MRI unit (Skyra Magnetom, version VE 11; Siemens Healthineers, Erlangen, Germany) by using an 18-channel phased-array body coil. All study participants were placed in the supine position with the arms along the body. Two three-dimensional, ultrashort–echo-time, gradient-echo spiral volume interpolated breath-hold examination (or VIBE) sequences, one following a full inspiration and the other after a full expiration, were acquired in all study participants. Each sequence, performed in the coronal plane, lasted 17 seconds. Parameters were as follows: repetition time, 2.73 msec; echo time, 0.05 msec; flip angle, 5°; field of view, 500 × 500 mm; section thickness, 2.5 mm; matrix, 240 × 240; in-plane resolution, 2.08 × 2.08 mm; spiral duration, 1800 μsec; and acceleration factor (iPAT; Siemens) of 2.

Elastic Registration

Following semiautomated lung segmentation with Myrian XP-Lung software (version 1.19.1; Intrasense, Montpellier, France), registration of inspiratory to expiratory images was performed by using an in-house multimetric, multimodal, graph-based elastic registration algorithm (9) (Fig 1).

This registration algorithm is available for research purposes at *https://www.mrf-registration.net*. Calculations were performed on a workstation with four graphic processing units (GTX1080; Nvidia, Santa Clara, Calif). To prepare for registration, all voxels outside the lung were masked out by using the same level of signal intensity of 400, close to that of chest wall muscles. This allowed obtaining a uniform background to avoid registration errors.

The quality of elastic registration was evaluated by comparing its performance to that of two independent observers (Fig E1 [online]). The first observer (C.M., with 1 year of experience in thoracic imaging) manually placed all landmarks on inspiration images and then on expiration images by using an open-source segmentation tool (ITK-SNAP; *http://www.itksnap.org*). A second observer (G.C., with 3 years of experience in thoracic imaging) directly placed the corresponding points on the expiratory images. Elastic registration automatically placed the landmarks of inspiratory images on expiratory images (registered expiratory landmarks). All expiratory landmark coordinates were collected and the mean distances were calculated as follows: distance A, between observer 1 and 2; distance B, between observer 1 and registered expiratory landmarks; and distance C, between observer 2 and registered expiratory landmarks.

Analysis of Lung Deformation

Elastic registration of inspiration to expiration produced diffeomorphic deformation maps for each study participant from which the Jacobian determinant of each voxel was calculated. The Jacobian determinant corresponds to the quantitative value of the volume change for each voxel of a Jacobian matrix. It quantifies the stretching or shrinking of each voxel (Fig 2). The Jacobian determinants were postprocessed as follows:

In step 1, the Jacobian determinants were normalized for each participant by using his or her own ratio of expiratory volume to inspiratory volume as a moderation factor. This ratio obtained from lung segmentations allowed taking into account the varying degrees of expiration among study participants and obtaining relative values of Jacobian determinants.

In step 2, expiratory MRI in one of the healthy volunteers was used as common template for Jacobian comparison in the entire cohort. Each participant's expiratory mask was registered to the common expiratory mask and the calculated transformation was applied to the Jacobian determinants.

In step 3, the Jacobian determinants were averaged to produce a unique three-dimensional Jacobian map for each group of study participants: study participants with SSc without pulmonary

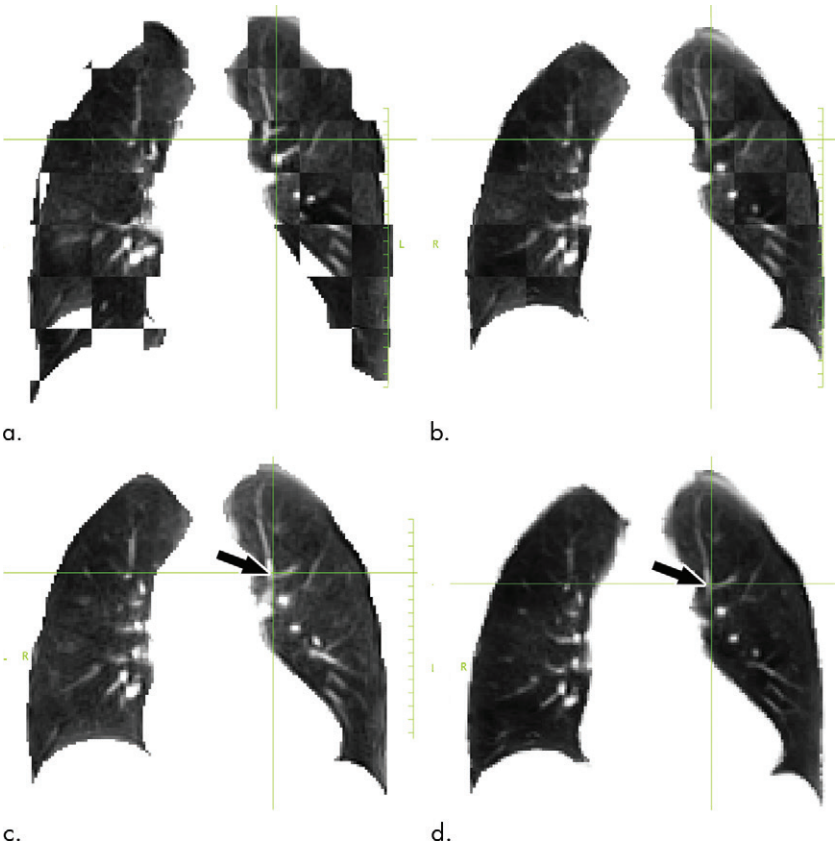

Figure 1: Images show example of inspiratory-to-expiratory elastic registration of coronal lung MRI in a healthy 24-year-old man using algorithm. **(a)** Checkboard image before elastic registration shows differences between source inspiratory image and target expiratory image. **(b)** Checkboard image after elastic registration. **(c)** Target expiratory image. **(d)** Inspiratory image after elastic registration. Arrows on vessel bifurcation in **c** and **d** show correct match between two images.

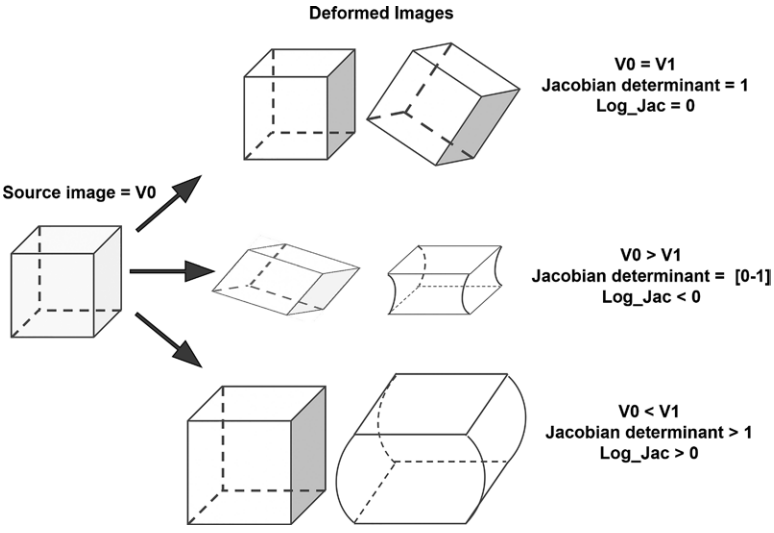

Figure 2: Illustration depicts Jacobian determinant. Jacobian determinant is quantitative value of deformation matrix of each voxel. If voxel size remains similar after deformation (V0 = V1), then Jacobian determinant is 1 and logarithm of Jacobian determinant (Log_Jac) is 0. If deformed voxel is smaller than original, then Log_Jac has negative value, whereas if deformed voxel is larger, then Log_Jac is positive.

fibrosis, study participants with SSc-related pulmonary fibrosis, and healthy volunteers.

In step 4, axial, sagittal, and coronal two-dimensional Jacobian maps were produced for each participant and each group by averaging Jacobian determinants along each axis (x, y, z) to represent the deformation on axial, coronal, and sagittal views.

Color maps were used to visually represent deformation based on the logarithm of the Jacobian determinants. Negative values indicated voxel shrinking, positive values indicated voxel stretching, and nil values indicated no volume change in the voxel (Fig 2). Based on the color maps, we defined lung areas showing marked shrinkage as those with Jacobian logarithm values below −0.15. Marked shrinkage areas were segmented for each study participant with SSc by using this cutoff value as a threshold, and they were compared with marked shrinkage areas of the unique three-dimensional Jacobian map for the healthy volunteer group. This comparison used the Dice similarity coefficient (10). The Dice similarity coefficient is a statistic used to compare the similarity of two samples, commonly used in image segmentation.

Statistical Analysis

All analyses were performed with XLSTAT software (version 19.4; Addinsoft, NY) and R software (version 3.3.3; R Foundation, Vienna, Austria). Characteristics of the study participants were compared by using the Fisher exact test for categorical variables or analysis of variance and Student t test for quantitative data. Distances between expiratory landmarks were compared by using the Bartlett variance test. Receiver operating characteristic analysis was used to determine the best cutoff values of Dice similarity coefficient for the presence of pulmonary fibrosis. P values $<.05$ were considered to indicate statistical significance.

Results

Study Population

Two of the 20 participants with SSc referred for routine cardiac MRI during the study period refused to participate and one participant (younger than 18 years) did not fulfill the inclusion criteria. Another participant was excluded because of poor quality of the MRI due to a misunderstanding of breathing instructions. Thus, 16 study participants with SSc were evaluated (Fig 3). Their high-resolution CTs were then reviewed by a thoracic radiologist (M.P.R., with 18 years of experience) who defined one group with and the other group

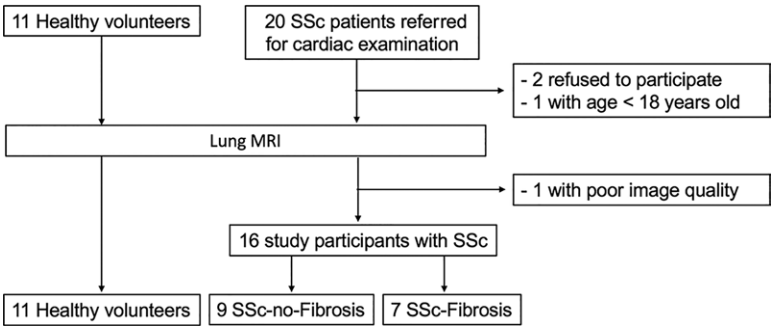

Figure 3: Flowchart shows study population. SSc = systemic sclerosis.

Study Cohort Characteristics

Characteristic	Healthy Volunteers (n = 11)	Systemic Sclerosis and No Fibrosis (n = 9)	Systemic Sclerosis and Fibrosis (n = 7)	P Value
Female sex	2 (18)	7 (78)	5 (71)	.02*
Age (y)†	29.1 ± 9.3	59 ± 17.5	60 ± 16.3	<.001*
Body mass index†	21.8 ± 1.6	22.6 ± 2.3	21.8 ± 2.9	.67*
Smoker	3 (27)	4 (44)	3 (42)	.68*
Forced vital capacity†‡	…	96 ± 26	66 ± 19	.03
DLCOc†‡	…	68 ± 15	38 ± 6	<.001

Note.—Unless otherwise specified, data are numbers of study participants, with percentages in parentheses. DLCOc = carbon monoxide–diffusing capacity corrected for anemia.

* Comparison of the three groups (healthy volunteers, study participants with systemic sclerosis without pulmonary fibrosis, and study participants with systemic sclerosis–related pulmonary fibrosis).

† Data are means ± standard deviation.

‡ Indicates percentage of predicted value.

without signs of SSc-related pulmonary fibrosis. A group of 11 healthy volunteers was also evaluated.

Thus, there were 27 study participants in total, 14 women and 13 men (Table). Women (mean age ± standard deviation, 54.8 years ± 19.2; range, 24–82 years) were significantly older than men (mean age, 38.8 years ± 19.1; range, 24–81 years) (P = .04).

At high-resolution CT, nine of the 16 study participants with SSc had no signs of infiltrative lung disease, whereas the remaining seven had signs of SSc-related pulmonary fibrosis with traction bronchiectasis in addition to ground glass and reticulations predominantly affecting the posterior portions of both lower lobes. The mean interval between MRI and high-resolution CT was 14 days ± 26. Healthy volunteers were more frequently men (P = .01) and younger than study participants with SSc. Forced vital capacity and carbon monoxide–diffusing capacity corrected for anemia values were poorer in participants in the SSc-related fibrosis group (P = .03 and P < .001, respectively) than in participants without pulmonary fibrosis. Body mass index did not differ among the three groups (P = .67).

Evaluation of Elastic Registration

The mean distance between the expiratory landmarks of observers 1 and 2 (distance A) was 7.4 mm ±7.1, whereas the mean distances between observers and registered landmarks (distance B and C) were 5.8 mm ± 5.1 and 7.7 mm ± 5.9, respectively. There was no statistical difference among the three mean distances (P = .49).

Visual Analysis of Lung Deformation

Visual analysis of color maps showed differences in the distribution of the Jacobian determinants among the study participants with SSc and healthy volunteers. The areas with marked deformation during expiration were found in the posterior part of the lung bases in healthy volunteers and in study participants with SSc without pulmonary fibrosis. The normalized Jacobian determinants did not demonstrate the same predominant expiratory deformation of the lung bases in study participants with pulmonary fibrosis (Fig 4).

Quantitative Analysis

Regarding the localization of marked shrinkage areas in the lung, the mean Dice similarity coefficient value was 0.44 ± 0.13 for study participants without fibrosis and 0.25 ± 0.15 for those with fibrosis (P = .02). Its best cutoff value for the presence of fibrosis was 0.36 at receiver operating characteristic curve analysis, with a sensitivity of 86% (95% confidence interval: 0.46, 0.99) and a specificity of 75% (95% confidence interval: 0.53, 0.89) (area under the curve, 0.81; 95% confidence interval: 0.54, 1) (P = .04) (Fig 5).

Discussion

This preliminary study evaluating elastic registration of inspiratory-to-expiratory MRI for the detection of pulmonary fibrosis in participants with systemic sclerosis (SSc) showed major visual differences in Jacobian maps between those with and those without fibrosis at high-resolution CT. There was a marked shrinkage of the lung bases during expiration in healthy volunteers and in study participants with SSc without fibrosis, but not in those with pulmonary fibrosis. So far, the evaluation of pulmonary fibrosis at MRI has mostly been based on gadolinium-enhanced sequences. Brady et al (11) evaluated late contrast enhancement, whereas Yi et al (12) performed contrast imaging at different times and showed differences in enhancement patterns between inflammatory and noninflammatory fibrotic lesions.

Currently, elastic registration methods are mainly used in radiation therapy to localize lesions and to generate phantoms of motion to anticipate cardiac or breathing movements (13,14). Recently, Han et al (15) described a registration method to estimate lung motion during a respiratory cycle on high-resolution CT images and follow the motion of lung nodules. The major drawback with CT is that the dose of radiation is doubled when both expiratory and

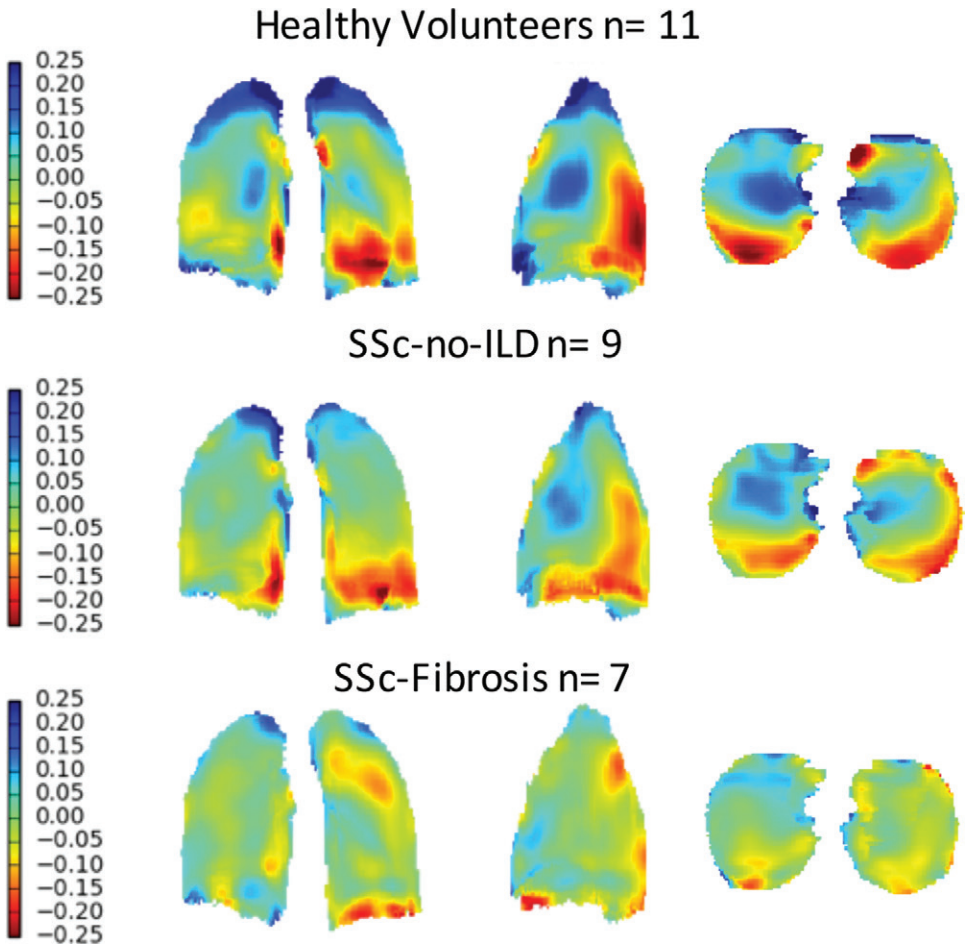

Figure 4: Images show projection in *x*, *y*, and *z* axis of mean of Jacobian determinants in each group. Marked shrinkage areas (in red) are found in dorsal aspect of lung bases in healthy volunteers and in study participants with systemic sclerosis (SSc) without evidence at high-resolution CT for pulmonary fibrosis. In corresponding areas, lungs of study participants with evidence for SSc-related fibrosis show little deformation with mean Jacobian determinant near to 0 (in green). These lung areas are those with signs of fibrosis at high-resolution CT.

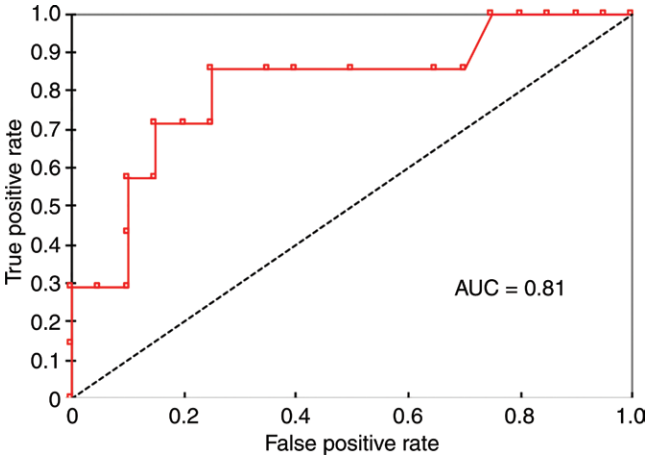

Figure 5: Graph shows receiver operating characteristic curve of Dice coefficient for entire cohort. Best Dice coefficient cutoff value for presence of fibrosis was 0.36, with sensitivity of 86% (95% confidence interval [CI]: 46, 99) and specificity of 75% (95% CI: 53, 89) (area under the curve [AUC], 0.81; 95% CI: 0.54, 1) (P = .04).

standard inspiratory acquisitions are performed, whereas MRI is radiation free. Sundaram et al (16), showed a difference in lung motion between healthy and hypoxemic mice by using MRI and elastic registration. We show that unenhanced MRI sequences, performed at the end of inspiration and expiration, can effectively and noninvasively help to detect lung fibrosis.

We observed the same expiratory deformation pattern in healthy volunteers and study participants with SSc without fibrosis, with a decrease in volume mainly found in the posterior lung bases. This was not observed in study participants with fibrosis. Under the assumption that a loss of elasticity might precede the appearance of fibrotic changes at high-resolution CT, we also included participants with SSc but no signs of infiltrative lung disease at high-resolution CT. However, this hypothesis was not confirmed in our sample.

There were several limitations to our study. First, this feasibility study only included a small number of study participants, resulting in large confidence intervals for sensitivity and specificity. Furthermore, healthy participants and participants with disease were not age and sex matched. For practical and ethical reasons, lung MRI sequences were not repeated to assess repeatability of the method. Also, we did not take into account the clinical scoring of skin sclerosis. Patients with high Rodnan skin scores (>20) (17) have marked skin sclerosis, which can result in decreased chest expansion. However, the lack of basal shrinkage in study participants with SSc-related fibrosis supports our hypothesis that this method effectively identifies fibrosis-related loss of elasticity, because restriction from skin sclerosis would not be predominantly basal. Finally, we only evaluated patients who could hold their breath for 17 secs; thus, this method is probably not applicable to patients with advanced lung disease.

In conclusion, elastic registration of inspiratory-to-expiratory MRI offers new perspectives in the noninvasive evaluation of lung fibrosis in patients with systemic sclerosis. These results must be confirmed in a larger cohort, but could apply to other fibrotic lung diseases.

Author contributions: Guarantors of integrity of entire study, G.C., C.M., L.M., M.P.R.; study concepts/study design or data acquisition or data analysis/interpretation, all authors; manuscript drafting or manuscript revision for important intellectual content, all authors; approval of final version of submitted manuscript, all authors; agrees to ensure any questions related to the work are appropriately resolved, all authors; literature research, G.C., C.M., R.M., A.R., L.M., N.P., M.P.R.; clinical studies, G.C., C.M., R.M., M.V., A.R., L.M., N.P.; statistical analysis, G.C., C.M., M.V., N.P.; and manuscript editing, G.C., C.M., R.M., A.R., L.M., N.P., M.P.R.

Disclosures of Conflicts of Interest: **G.C.** disclosed no relevant relationships. **C.M.** Activities related to the present article: received a research grant from French Society of Radiology and CARDIF Foundation. Activities not related to the present article: disclosed no relevant relationships. Other relationships: disclosed no relevant relationships. **R.M.** Activities related to the present article: disclosed no relevant relationships. Activities not related to the present article: is an employee of TheraPanacea; institution received payment from École CentraleSupelec for intellectual property. Other relationships: disclosed no relevant relationships. **M.V.** disclosed no relevant relationships. **A.R.** disclosed no relevant relationships. **L.M.** disclosed no relevant relationships. **N.P**. Activities related to the present article: institution received payment for grants from Agence Nationale de la Recherche, European Research Council, and Horizon 2020. Activities not related to the present article: is partially affiliated with TheraPanacea; has grants/grants pending with Agence Nationale de la Recherche and Horizon 2020; receives royalties for intellectual property from CentraleSupelec; owns stock/stock options in TheraPanacea. Other relationships: institution received payment from École CentraleSupelec for intellectual property. **M.P.R.** disclosed no relevant relationships.

References

1. Behr J, Furst DE. Pulmonary function tests. Rheumatology (Oxford) 2008;47(Suppl 5):v65–v67.
2. Johnson KM, Fain SB, Schiebler ML, Nagle S. Optimized 3D ultrashort echo time pulmonary MRI. Magn Reson Med 2013;70(5):1241–1250.
3. Ohno Y, Koyama H, Yoshikawa T, Seki S. State-of-the-art imaging of the lung for connective tissue disease (CTD). Curr Rheumatol Rep 2015;17(12):69.
4. Dournes G, Grodzki D, Macey J, et al. Quiet submillimeter MR imaging of the lung is feasible with a PETRA sequence at 1.5 T. Radiology 2015;276(1):258–265.
5. Roach DJ, Crémillieux Y, Serai SD, et al. Morphological and quantitative evaluation of emphysema in chronic obstructive pulmonary disease patients: A comparative study of MRI with CT. J Magn Reson Imaging 2016;44(6):1656–1663.
6. Delacoste J, Chaptinel J, Beigelman-Aubry C, Piccini D, Sauty A, Stuber M. A double echo ultra short echo time (UTE) acquisition for respiratory motion-suppressed high resolution imaging of the lung. Magn Reson Med 2018;79(4):2297–2305.
7. McClelland JR, Hawkes DJ, Schaeffter T, King AP. Respiratory motion models: a review. Med Image Anal 2013;17(1):19–42.
8. van den Hoogen F, Khanna D, Fransen J, et al. 2013 classification criteria for systemic sclerosis: an American College of Rheumatology/European League against Rheumatism collaborative initiative. Arthritis Rheum 2013;65(11):2737–2747.
9. Glocker B, Sotiras A, Komodakis N, Paragios N. Deformable medical image registration: setting the state of the art with discrete methods. Annu Rev Biomed Eng. 2011;13:219–244.
10. Dice LR. Measures of the amount of ecologic association between species. Ecology 1945;26(3):297–302.
11. Brady D, Lavelle LP, McEvoy SH, et al. Assessing fibrosis in pulmonary sarcoidosis: late-enhanced MRI compared to anatomic HRCT imaging. QJM 2016;109(4):257–264.
12. Yi CA, Lee KS, Han J, Chung MP, Chung MJ, Shin KM. 3-T MRI for differentiating inflammation- and fibrosis-predominant lesions of usual and nonspecific interstitial pneumonia: comparison study with pathologic correlation. AJR Am J Roentgenol 2008;190(4):878–885.
13. Zhang Y, Yang J, Zhang L, Court LE, Balter PA, Dong L. Modeling respiratory motion for reducing motion artifacts in 4D CT images. Med Phys 2013;40(4):041716 [Published correction appears in Med Phys 2015;42(11):6768.].
14. Liu F, Hu Y, Zhang Q, Kincaid R, Goodman KA, Mageras GS. Evaluation of deformable image registration and a motion model in CT images with limited features. Phys Med Biol 2012;57(9):2539–2554.
15. Han L, Dong H, McClelland JR, Han L, Hawkes DJ, Barratt DC. A hybrid patient-specific biomechanical model based image registration method for the motion estimation of lungs. Med Image Anal 2017;39:87–100.
16. Sundaram TA, Gee JC. Towards a model of lung biomechanics: pulmonary kinematics via registration of serial lung images. Med Image Anal 2005;9(6):524–537.
17. Rodnan GP, Lipinski E, Luksick J. Skin thickness and collagen content in progressive systemic sclerosis and localized scleroderma. Arthritis Rheum 1979;22(2):130–140.